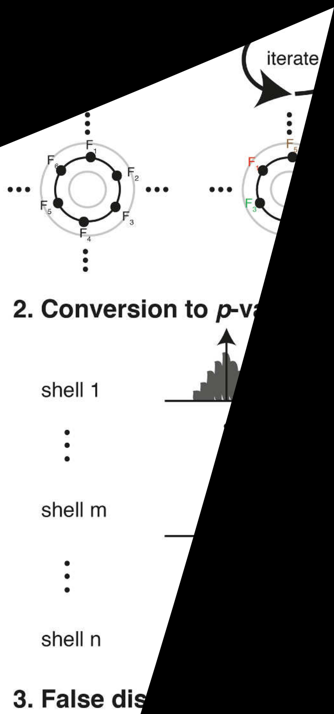

[redacted]

Fig. 1. Resolution estimati [redacted]
creating newly paired Fou [redacted]
for the original FSC valu [redacted]
Histograms of permuted [redacted]
(c) Comparison of the e [redacted]
and subsequent FSC ca [redacted]
σ-threshold criteria a [redacted]
closely, especially at [redacted]

has a certain sign [redacted]

As an altern [redacted]
provide cutof [redacted]
(Saxton and [redacted]
curve gives [redacted]
compare it [redacted]
tion of vo [redacted]

$\sigma(r_i) =$ [redacted]

σ_r [redacted]
thre [redacted]
σ_{m} [redacted]
(C [redacted]
S [redacted]

[redacted] g
[redacted] nly
[redacted] of a
[redacted] emove
[redacted] elations.
[redacted] on (Chen
[redacted] volves em-
[redacted] hile avoiding
[redacted] the absence of
[redacted] unmasked FSC
[redacted] of unmasked and
[redacted] mass have been pro-
[redacted] Grigorieff, 2012), such
[redacted] FSC threshold. Here, we
[redacted] resolution determination

[redacted] testing of F [redacted]

[redacted] umvent principal and p [redacted]
[redacted] urves, we developed a procedu [redacted]
[redacted] ation shell of interpretable signal b [redacted]
mutation sampling and subsequent stat [redacted]
tests are statistical procedures for est [redacted]
quantity of interest from the data itse [redacted]
prior knowledge about the underlyi [redacted]
Romano, 2005). Permutation samplin [redacted]
shell is straightforward: we generat [redacted]
order of the Fourier coefficients [redacted]
compute a large series of FSCs (Fi [redacted]
existing correlations between Four [redacted]
therefore, yield a sample of the [redacted]
resolution shell. When applied t [redacted]
tions together with the origina [redacted]
tested and conveniently transf [redacted]
invariant to the color of the n [redacted]
independently and we do not [redacted]
tribution. When we test mult [redacted]
higher risk of falsely identif [redacted]
make a false positive disc [redacted]
testing problem in statisti [redacted]
errors, *p*-values are fu [redacted]
(Benjamini and Hochbe [redacted]
term this approach the [redacted]

2.2. Permutation samp [redacted]

In order to veri [redacted]
principal distribut [redacted]
two pure noise re [redacted]
deviation of 1 a [redacted]
assess the true [redacted]
lated 5000 noi [redacted]
deviation of [redacted]
maps. Comp [redacted]
generated f [redacted]
pixel) and [redacted]
tions (EQ [redacted] se
proach a [redacted] the
of the [redacted] of the
standa [redacted] on the
one [redacted] threshold
nois [redacted] of resolu-
m [redacted] we routinely
d [redacted] cutoff to the
[redacted] resolution band

[redacted] *on FSC permutation*

[redacted] king and symmetrization

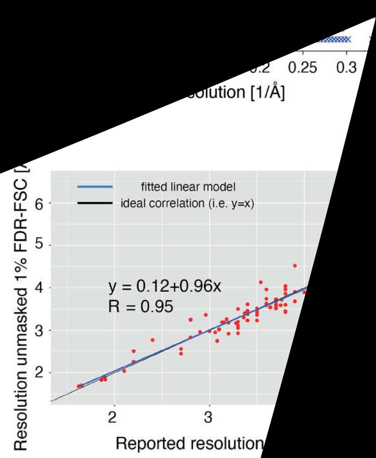

Fig. 2. Effects of surrounding solve [redacted] correlation (FSC) curve for γ-scret [redacted] beyond random fluctuations at 1% [redacted] on FSC curve by decreasing win [redacted] estimates at 0.143 FSC (blue) co [redacted] Fitted line (R = 0.95) is shown [redacted] values. (f) Two histograms of [redacted]

applied to both half-map [redacted] shells. These principal [redacted] sequences for threshold [redacted] were proposed to be c [redacted] Schatz, 2005). Introdu [redacted] a shell affect the dis [redacted] outlined permutatio [redacted] plied to the image [redacted] be correlated rega [redacted] standard FSC per [redacted] maps, depende [redacted] narrower distri [redacted] such symmetr [redacted] described by [redacted] involved in [redacted] freedom o [redacted] corefficie [redacted] quired t [redacted] shell.

In [redacted] ident [redacted] 10-f [redacted] EM [redacted] c [redacted]

[redacted] ly [redacted] osed [redacted] re re- [redacted] e used [redacted] oks et al., [redacted] ults match [redacted] mmetry: 2.9 [redacted] reported) and [redacted] he latter test of [redacted] mple size correc- [redacted] ter resolution than [redacted] t taking into account [redacted] for FSC computation is [redacted] ng and can be efficiently [redacted] ection in the permutation

[redacted] Gaussian [redacted] is not [redacted] map operation. [redacted] size for the effect [redacted] the deviation between the [redacted]
5000 noise half-maps (with [redacted]
distribution calculated from two noise [redacted]
sphere applied) by permutation [redacted]
systematically testing different [redacted]
the Kolmogrow-Smirnow distance [redacted]
1951) (see Methods for more details). [redacted]
sphere reduces the effective [redacted]
size (Supplementary Fig. 5a). We [redacted]
as it is used for local resolution [redacted]
sample size correction factor ([redacted]
effective sample sizes is [redacted]
and simulated percentiles using [redacted]
resulting percentile lines [redacted]
sample sizes are considered ([redacted]
noted that the tests also [redacted]
mask for solvent flattening [redacted]
tation sampling of the [redacted]
commended in the [redacted]
factor.

After assessing the [redacted]
with regards to [redacted]
maps containing [redacted]
need to be [redacted]
corrections, e.g. in [redacted]
comes 1/4 times [redacted]
approach, we [redacted]
imposed [redacted]
sizes. In [redacted]
compared the [redacted]
noise [redacted]
percentiles as [redacted]
effective [redacted]
to tail [redacted]
symmetry. [redacted]
however, [redacted]
fective [redacted]
erations [redacted]
as [redacted]

[redacted]	FDR-FSC [Å]
[redacted]	6.48
[redacted]	8.05
[redacted]	11.03
[redacted]	5.0
[redacted]	21.68
[redacted]	21.68
[redacted]	13.1
[redacted]	23.29
[redacted] 6.77	6.32

[redacted] DB II [redacted]
[redacted] solutions o [redacted]
[redacted] dard deviation of [redacted]
[redacted] se (Supplementary Fig. [redacted]
[redacted] om overlapping cubes includi [redacted]
[redacted] dimension followed by permutati [redacted]
spective sample size correction facto [redacted]
thresholding, we determined local reso [redacted]
noise levels that ranges in standard dev [redacted]
comparison, the commonly used 0.5 lo [redacted]
differences to the simulated resolution [redacted]
to give lower resolutions in comparis [redacted]
at low noise levels (Supplementary [redacted]
mental 3.4 Å γ-secretase map (Bai e [redacted]
the 1% FDR-FSC criterion assigns [redacted]
solved core of the membrane prot [redacted]
cutoff, while at the same time, lo [redacted]
are found at peripheral glycosyl [redacted]
top left). Both observations ca [redacted]
density features and are thus f [redacted]
estimation method. An impor [redacted]
solution shells included in [redacted]
window size. In order to tes [redacted]
we computed the local reso [redacted]
local threshold FSC metho [redacted]
(Bai et al., 2015) (EMD30 [redacted]
50 pixels (Supplementar [redacted]
15), we observe too [redacted]
sampling, whereas for [redacted]
stant resolution value [redacted]
(Supplementary Fig. [redacted]
is estimated worse t [redacted]
threshold yields a r [redacted]
features of the cr [redacted]
responding to th [redacted]
spect to window [redacted]
the window si [redacted]
lower spatial [redacted]
of resolution [redacted]
formation fr [redacted]
resolved tr [redacted]
gets bette [redacted]
Taken to [redacted] ex-
proach. [redacted] o-EM
chose [redacted] ut deli-
suffic [redacted] roach of
[redacted] sampling
loc [redacted] pproach was
cr [redacted] map thresh-
[redacted] es not have any
[redacted] volume symmetry
[redacted] truction. This way,
[redacted] tion without solvent
[redacted] f generating tight user-
[redacted] volution process (Chen
[redacted] ches have been proposed

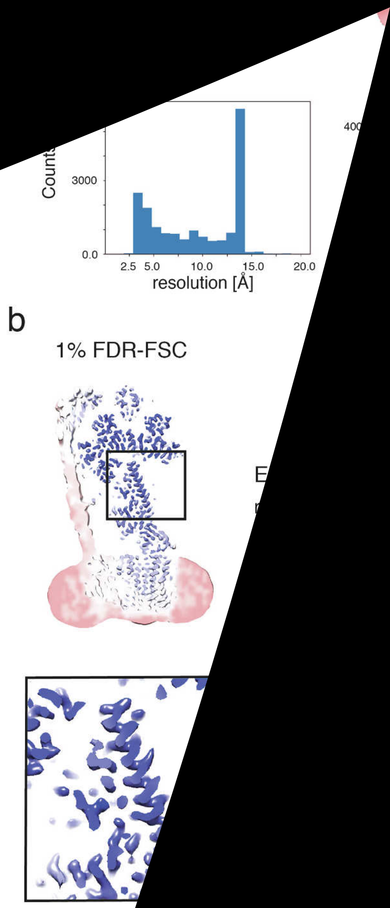

Fig. 3. Application [redacted]
FSC, ResMap and M[redacted]
3.9 Å map of a ba[redacted]
3.8 Å map of a e[redacted]

(Sindelar and [redacted]
molecular v[redacted]
routinely a[redacted]
heterogen[redacted]
mation s[redacted]ise
capture[redacted]s per
tures a[redacted]e little
Comp[redacted]er shell.
lyze[redacted]dependent
ani[redacted]erimentally
p[redacted]y introduced
s[redacted]ngle resolution
[redacted]he FSC. Common
[redacted]ng within the re-
[redacted], and as a result the
[redacted]uced and the true FSC
[redacted]y subsampling. We im-
[redacted]sample size to capture the

[redacted]

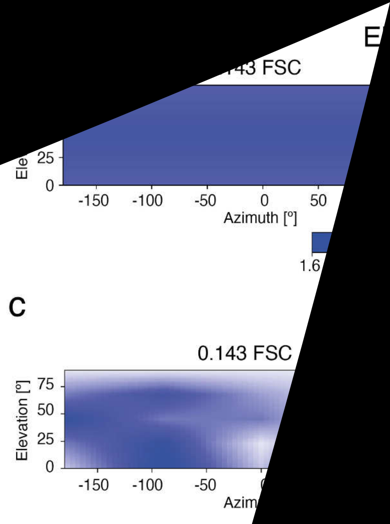

[redacted]

Fig. 4. Application of FDR-FSC [redacted] (b) apoferritin (EMD0144) and [redacted] directions corresponding to a[redacted] voxel specifies the resolutio[redacted] differences are reported usi[redacted]

true FSC value distribu[redacted] nominal sample size w[redacted] maps are introduced [redacted] masks, mis-alignme[redacted] components such a[redacted] to the 3D reconst[redacted] half-maps. These [redacted] permutation sam[redacted] the applied ima[redacted] sing work-flow[redacted] different part[redacted] omitting hig[redacted] finement i[redacted] pendencie[redacted]n

Once [redacted]les of the [redacted]ns. Finally [redacted]e pro- step. [redacted]ne com- diffe[redacted]ibute this add[redacted]e of solvent tis[redacted]ze remains a n[redacted] resolutions re-[redacted]eing used (see [redacted]y when local FSC [redacted]rom the respective [redacted] in detail previously [redacted]dow size, the here pre-[redacted]er 0.5 FSC, as it is less

[redacted] isual [redacted] es. For futu [redacted] used as an additi [redacted] her standard validation [redacted] bustness, we see particular u [redacted] mination into more challenging ap [redacted]
directional resolution where resolution [redacted]
interpretation but technically less stand [redacted]
script, we presented the FDR-FSC metho [redacted]
evaluation. It has to be noted that the p [redacted]
to 2D Fourier ring correlations as use [redacted]
(Nieuwenhuizen et al., 2013). Due to [redacted]
robustness, we anticipate a comm [redacted]
method to image analysis and proce [redacted]
EM field.

4. Methods

4.1. Permutation sampling of Fo [redacted]

We consider X_{r_i} and Y_{r_i} t [redacted]
denote the corresponding Fo [redacted]
$i = 1, \cdots, N$, in resolution s [redacted]
the number of Fourier coeff [redacted]
symmetry, there are n [redacted]
Correlations between X_r [redacted]
position r_i, which we de [redacted]
maps. Thus, Fourier co [redacted]

$X_{r_i} = S(r_i) + N_X(r_i)$an [redacted]

where $N_X(r_i)$ and N_Y [redacted]
and Schatz, 2005). [redacted]
in resolution sh [redacted]
$X_R = (X_{r_1}, \cdots, X_{r_n})$ [redacted]
Fourier coefficie [redacted]

We design [redacted]
nificant Fourie [redacted]
for two half- [redacted]
Fourier coef [redacted]
correlated [redacted]
location r_i [redacted]
pothesis [redacted]
hypothe [redacted]
tions a [redacted]
is, usi [redacted]
valu [redacted]

FS [redacted]

[redacted] ells sepa-
[redacted] lly simply
[redacted] ommonly re-
[redacted] e significance
[redacted] respect to FSC
[redacted] number of tested
[redacted] 20 for windows of
[redacted] complete maps. As a
[redacted] at put individual sig-
[redacted] nificance level have been
[redacted]). In particular, the false

[redacted] *masking*

[redacted] in the Results section, [redacted] symmetrization of the [redacted] Fourier coefficients and thus [redacted] freedom. Due to dependencies, the [redacted] sample of independent realizations of [redacted] Carlo simulations this smaller sample [redacted] effective sample size n_{eff}. The [redacted] metry during reconstruction can be [redacted]

$$n_{eff} = \frac{n}{n_{as}}$$

where n is the number of Fourier [redacted] tion shell and n_{as} is the number [redacted] symmetry (Supplementary Fig. [redacted] corporated in the permutation [redacted] coefficients in the respective [redacted] or masking on the effective [redacted] pend on the specific shape [redacted] sample size of the complete [redacted] the effective sample size [redacted]

through minimization of [redacted] over the resolution [redacted] tance (Massey, 1951), [redacted] larity of two [redacted] difference between the [redacted] (ECDF). The ECDF [redacted] smaller or equal to [redacted] probability of [redacted] tween these [redacted] observed for any [redacted]

In our case [redacted] correction [redacted] then given as: [redacted]

$D_{\alpha,r} = \sup$ [redacted]

where in [redacted] approach [redacted] of [redacted] FSC [redacted]

[redacted] previously [redacted] a GUI based [redacted] cryo-EM maps [redacted] based on NumPy [redacted]), SciPy (Oliphant, [redacted] by the Python [redacted] able at https://github. [redacted] prepared with UCSF

grateful to Thomas Hoffmann
maintenance of the high-performance

Appendix A. Supplementary data

Supplementary data to this article
doi.org/10.1016/j.jsb.2020.107579.

References

Bai, X.C., Yan, C., Yang, G., Lu, P., Ma, D.,
2015. Nature 525, 212–217.
Banterle, N., Bui, K.H., Lemke, E.A., Beck
Bartesaghi, A., Merk, A., Banerjee, S., M
S., 2015. Science (80-.) 348, 1147–
Beckers, M., Jakobi, A.J., Sachse, C., 2
Benjamini, Y., Hochberg, Y., 1995. J.
Benjamini, Y., Yekutieli, D., 2001. An
Brooks, S., Gelman, A., Jones, G.L., M
Carlo. Chapman & Hall.
Burnley, T., Palmer, C.M., Winn, M
469–477.